Radiopaque poly(ε-caprolactone) as additive for X-ray imaging of temporary implantable medical devices — Source link ☐

Rémi Samuel, Edouard Girard, Edouard Girard, Grégory Chagnon ...+6 more authors

Institutions: University of Montpellier, Centre national de la recherche scientifique, University of Grenoble

Related papers:

- Synthesis of an X-ray opaque biodegradable copolyester by chemical modification of poly (epsilon-caprolactone).

- Non-invasive deep tissue imaging of iodine modified poly(caprolactone-co-1-4-oxepan-1,5-dione) using X-ray.

- Non-invasive monitoring of in vivo degradation of a radiopaque thermoreversible hydrogel and its efficacy in preventing post-operative adhesions.

- Characterisation of blends between poly(ε-caprolactone) and polysaccharides for tissue engineering applications

- An injectable thermogel with high radiopacity

Radiopaque poly(e-caprolactone) as additive for X-ray imaging of temporary implantable medical devices

Rémi Samuel, Edouard Girard, Grégory Chagnon, Stéphane Dejean, Denis Favier, Jean Coudane, Benjamin Nottelet

Radiopaque poly(3-caprolactone) as additive for X-ray imaging of temporary implantable medical devices

Rémi Samuel,[a] Edouard Girard,[bcd] Grégory Chagnon,[cd] Stéphane Dejean,[a] Denis Favier,[cd] Jean Coudane[a] and Benjamin Nottelet[*a]

Implantable polymeric medical devices suffer from a lack of visibility under current clinical imaging techniques. To circumvent this problem, poly(ε-caprolactone-*co*-α-triiodobenzoate-ε-caprolactone)s (PCL-TIB) containing from 3.5% to 24% of triiodobenzoate-ε-caprolactone units were synthesized as new X-ray macromolecular contrast agents. Physico-chemical and thermal properties of PCL-TIBs were evaluated by ^{1}H NMR, SEC, DSC and TGA. Their potential as radio-opacifying additive for medical devices was evaluated by preparing polymeric blends of PCL-TIB with various (co)polyesters. At first, *in vitro* X-ray visibility of PCL/PCL-TIB blends was evaluated. A more in depth characterization was then carried out based on PCL/PLA$_{50}$-PEG-PLA$_{50}$ blends. The impact of PCL-TIB content on the mechanical properties of blends was evaluated by tensile tests. Stability of X-ray visibility was evaluated by *ex vivo* implantation of non-degraded blends and of blends degraded for 6 weeks *in vitro*. Finally, cytocompatibility was assessed by evaluating the proliferation of L929 fibroblasts on the blends.

Introduction

Medical imaging has a strong impact on modern medicine practice and participates to the raise of advanced applications including *in vivo* cell marking, early diagnosis of diseases, image-guided therapy or post-surgical medical devices follow-up.[1,2] This is in particular the case of X-ray imaging, a low cost imaging technique that has been used for over a century and provides good spatial resolution with no limit on tissue penetration depth. In the early 70's, X-ray computed tomography (CT) was developed to produce cross-sectional images of the body. The mechanism of CT imaging is based on the absorption of X-rays as they pass through tissues with distinct degrees of attenuation that depend on the atomic number and electron density of the tissues.[3] The differences in absorption between bone, fat, water, and air yield high contrast images of anatomical structures. To achieve a signal that is sufficient for clinical purposes, contrast agents (CAs) are however generally required. The principle of CAs is to increase the signal to noise ratio (SNR) relative to surrounding tissues to provide clear discrimination between normal and pathological regions in areas of interest.[1] CAs are therefore found in all molecular imaging modalities currently in use, including X-ray radiography/computed tomography (CT). Classical low molecular weight CT CAs or radio-opacifying agents include gold nanoparticles, heavy metal powders (tantalum), inorganic salts of heavy elements (barium sulfate, bismuth sulfide), or organic compounds containing a heavy atom (iodine).[4–6] Small-molecular mass CAs are however characterized by rapid extravasation and clearance. They are also known to induce recurrent problems like acute renal toxicity or adverse allergic and pseudo-allergic reactions.[4,7] These factors, in addition to the ionizing character of X-ray, explain that X-ray imaging still represents today only *ca.* 7% of the medical images.

A renewed and strong interest is however currently witnessed based on two approaches. The first one is the development of micro-computed tomography (μCT) application to soft tissues, where specific X-ray CAs with a selective biodistribution have been designed.[8,9] The second one is the development of macromolecular CAs.[10,11] Indeed, polymeric biomaterials featuring radio-opacity attract considerable scientific attention since it is highly desirable to visualize medical devices such as cardiovascular implants, prostheses, orthopedic implants *via* routine X-rays computed tomography. In that frame, aliphatic polyesters are among the most common degradable polymers used in medical applications. Aliphatic polyesters include the

[a]Institute of Biomolecules Max Mousseron (IBMM) UMR 5247, Department of Arti*f*icial Biopolymers, CNRS, University of Montpellier, ENSCM, Faculté de Pharmacie, 15 avenue Charles Flahault BP14491, 34093 Montpellier Cedex 5, France.
[b]CHU de Grenoble, TIMC-IMAG, F-38000 Grenoble, France
[c]Université Grenoble Alpes, TIMC-IMAG, F-38000 Grenoble, France
[d]CNRS, TIMC-IMAG, F-38000 Grenoble, France

well-known poly(lactide) (PLA), poly(glycolide) (PGA), poly-(ε-caprolactone) (PCL) and their copolymers, like poly(lactic-*co*-glycolic acid) (PLGA). This family of polymers has been a first choice for a variety of biomedical applications, ranging from surgical suture to implants or drug nanocarriers.[12,13] This success story originated during the resorbable-polymer-boom of the 1970s and 1980s and is mostly due to their demonstrated biocompatibility and biodegradability that led to their validation by the regulatory agencies worldwide. Aliphatic polyesters and their copolymers are thermoplastics that present numerous advantages like tailorable degradation kinetics and mechanical properties, ease of shaping and manufacture. Their broad spectrum of properties can easily be tuned by the use for instance of lactic acid-based stereocopolymers, or copolymerization with the biocompatible hydrophilic poly(ethylene glycol) (PEG).[14,15] This is therefore not surprising to find them as core materials in the innovation pipeline of medical imaging strategies.

However aliphatic polyesters, as most polymeric biomaterials, are transparent to X-rays. They are generally made radiopaque by addition of an X-ray absorbing additive such as metal powders, metal salt based on tantalum, barium, bismuth, gold *etc.*[16–19] For example Lamsa *et al.* reported on a radiopaque stent composed of PLA96 with 25 wt% of $BaSO_4$ that was used as radiopaque bioabsorbable biliary stents.[20,21] To avoid leaching of potentially metallic compounds, organic–inorganic hybrids were also prepared *via* the sol–gel process starting from a dihydroxy-terminated polyester poly(1,4-butyleneglutarate) (PBG), PLA or PCL and a titanium alkoxide (TIPT) as titanium precursors.[22] It was demonstrated that a transesterification reaction of the polymer chain occurring *in situ* led to organotitanium esters connecting organic and inorganic domains that demonstrated radio-opacity.[23]

To circumvent the problem of potential toxicity encountered with metallic additives,[24] organic radio-opacifiers containing heavy atoms such as bromine or iodine were also proposed. However, the resulting polyester/radio-opacifier blends also suffer from leaching problems that result in the loss of imaging capabilities and potential toxicities. To avoid leaching, Koole *et al.* reported recently on biocompatible and PLA-miscible iodinated contrast agent, namely (*S*)-2-hydroxy-3-(4-iodobenzyloxy) propanoic acid that has a plasticizing effect due to structural compatibility with PLA.[25] The blend obtained with 10 wt% contrast agent yielded about 25% attenuation compared to aluminum. However, although blend compatibility was improved, no covalent bond was still found between the PLA backbone and the organic opacifier.

To achieve this goal, two strategies are described. The first one relies on covalent grafting of radio-opacifiers to polymer backbone in a post-polymerization modification strategy. In a second approach, iodinated monomers are copolymerized to yield radiopaque copolymers. These methodologies have been applied to various polymeric materials including cellulose,[26,27] poly(meth)acrylates,[3,28–35] polyurethanes,[6,36,37] polyphosphazenes[38] or polycarbonates.[39] However, only few studies report on aliphatic polyesters conjugates for X-ray modalities. To the best of our knowledge, the first radiopaque polyester bearing iodine was described by our group.[40] Poly(ε-caprolactone-*co*-α-iodo-ε-caprolactone) (PCL-I) was synthesized by introducing iodine in the α position of the carbonyl group of PCL thanks to an anionic activation of PCL followed by substitution with iodine. Copolyesters containing from 10% to 25% of iodized-units were thus obtained. In another strategy iodinated PCLs were prepared by copolymerization of α-iodo-ε-caprolactone with ε-caprolactone.[41,42] The X-rays opacity was assessed, and appeared high enough to be of interest for biomedical applications although stability of aliphatic carbone–iodine bond could be improved. More recently, Olsen *et al.* reported on the copolymerization of ε-caprolactone and 1,4,8-trioxaspiro-[4,6]-9-undecanone to yield after oxime ligation a copolyester containing 13% of iodized-units.[43] However, limited thermal stability of oxime grafts was reported. Other radiopaque biodegradable polyesters have been prepared by ring-opening polymerization of lactide and ε-caprolactone using an iodinated initiator, namely 2,2-bis(hydroxymethyl)propane-1,3-diyl bis(2,3,5-triiodobenzoate).[44] The resulting polyesters exhibited a radio-opacity of 60–124% relative to an aluminum sample of the same thickness and could be electrospun into nanofibers. Similarly, biodegradable radiopaque iodinated poly(ester-urethane) based on PCL oligomers and iodinated bisphenol containing up to 30 wt% iodine,[45] or salicylate-based poly(anhydride-ester),[46] have been reported. It should be noted that, whereas attenuation similar or even higher than aluminum and good cytocompatibility were shown with the poly(ester-urethane)s, cytotoxicity was observed towards L929 mouse fibroblasts with the iodinated salicylate-based poly(anhydride-ester)s.

Considering this limited number of radiopaque copolyesters available, and keeping in mind temporary implantable medical device as a final application, we aim in this work at providing a new radiopaque PCL for X-ray imaging with improved stability with respect to poly(ε-caprolactone-*co*-α-iodo-ε-caprolactone) (PCL-I). The synthesis of poly(ε-caprolactone-*co*-α-triiodobenzoate-ε-caprolactone) (PCL-TIB) based on anionic activation and post-polymerization modification of PCL is first described. Thermal properties and stability compared to PCL-I are then discussed before evaluation of PCL-TIB cytocompatibility towards L929 fibroblasts. Finally, the potential of PCL-TIB as macromolecular radio-opacifier is assessed through the preparation of blends of PCL-TIB and PLA-PEG copolymers. Blends have been characterized in terms of mechanical and imaging properties with in particular evaluation of the X-ray visibility *ex vivo* over a 6 weeks degradation period.

Experimental part

Materials

PCL ($\overline{M_n} \approx 32\,000$ g mol^{-1}), 2,3,5-triiodobenzoic acid (TIBA, 98%), thionyl chloride (97%), lithium diisopropylamide (LDA, 2 M in THF/heptane/ethylbenzene), were purchased from Sigma-Aldrich (St-Quentin Fallavier, France). NH_4Cl (>99%) was obtained from Acros Organics (Noisy-le-Grand, France), technical grade $MgSO_4$ from Carlo Erba (Val de Reuil, France), methanol (MeOH, ≥99.8%), dichloromethane (DCM, ≥99.9%) and anhydrous tetrahydrofuran (THF, ≥99.9%) from Sigma-

Aldrich (St-Quentin Fallavier, France). THF was distilled on benzophenone/sodium until a deep blue color was obtained. PrestoBlue™, Dulbecco's Modified Eagle Medium (DMEM/F-12), Phosphate Buffered Saline (PBS), sterile Dulbecco's Phosphate Buffered Saline (DBPS), Fetal Bovine Serum (FBS), penicillin, streptomycin, and glutamine were purchased from Invitrogen (Cergy Pontoise, France). BD Falcon™ Tissue Culture Polystyrene (TCPS) 24-well plates were purchased from Becton Dickinson (Le Pont de Claix, France) and Viton® O-rings from Radiospares (Beauvais, France).

Characterizations

The number average molecular weight ($\overline{M}_n$) and dispersity ($Đ$) of the polymers were determined by size exclusion chromatography (SEC) using a Waters 515 HPCL pump fitted with a PLGel 5 μm mixed C pre-column (50 × 7.5 mm) a PLGel 5 μm mixed C column (600 × 7.5 mm) and a Waters 410 refractive index detector. The mobile phase was $CHCl_3$ at 1 mL min^{-1} flow and 25 °C. Typically, the polymer (5 mg) was dissolved in $CHCl_3$ (1 mL), and the resulting solution was filtered through a 0.45 μm Millipore filter before injection of 20 μL of filtered solution. M_n was expressed according to calibration using polystyrene standards.

For stability studies, polymers were analyzed by SEC using a Waters 515 HPCL pump fitted with a PLgel 5 μm Guard column (50 × 7.5 mm), a PLGel 10 μm 500 Å columns (600 × 7.5 mm), a PLGel 10 μm 50 Å columns (300 × 7.5 mm), Waters 2410 refractive index detector and Waters 2996 photodiode array detector. The mobile phase was THF at 1 mL min^{-1} flow and 25 °C. Typically, the polymer (5 mg) was dissolved in THF (1 mL), and the resulting solution was filtered through a 0.45 μm Millipore filter before injection of 20 μL of filtered solution.

^{1}H NMR spectra were recorded at room temperature using an AMX300 Bruker spectrometer operating at 300 MHz. Deuterated chloroform was used as solvent, chemical shifts were expressed in ppm with respect to tetramethylsilane (TMS).

The thermal properties of the polymers were characterized by differential scanning calorimetry (DSC) and thermogravimetric analysis (TGA). DSC measurements were carried out under nitrogen on a Perkin-Elmer Instrument DSC 6000 Thermal Analyzer. Samples were submitted to a first heating scan from 20 °C to 110 °C (10 °C min^{-1}) followed by a cooling ramp to −65 °C (5 °C min^{-1}) followed by an isotherm at −65 °C (10 min) and a second heating ramp to 180 °C (5 °C min^{-1}). Melting temperature (T_{m_1}) and melting enthalpy (ΔH_{m_1}) were measured on the first heating ramp. Crystallization temperature (T_c) was measured on the cooling ramp. Melting temperature (T_{m_2}), melting enthalpy (ΔH_{m_2}) and glass transition temperature (T_g) were measured on the second heating ramp. TGA thermograms were obtained under normal atmosphere on a Perkin-Elmer Instrument TGA 6 at a scanning rate of 10 °C min^{-1} from 30 to 400 °C.

Synthesis of triiodobenzoyl chloride (TIBC)

2,3,5-Triiodobenzoyl chloride (TIBC) was obtained by reaction of 2,3,5-triiodobenzoic acid (TIBA) with thionyl chloride. In a typical experiment, TIBA (5 g, 10 mmol) was dissolved in thionyl chloride (50 mL) and the solution was heated to reflux under stirring for 16 hours. Excess thionyl chloride was distilled off under reduced pressure. Brown solid was obtained and purified by crystallization from hot tetrachloromethane. The resulting white solid needles were filtered and dried under vacuum. TIBC (60% yield) was characterized by NMR and FT-IR analyses (ESI Fig. S1 and S2†). FT-IR: acyl chloride band at 1759 cm^{-1}. ^{1}H NMR (300 MHz; CDCl$_3$): δ (ppm) = 7.9 and 8.3 (s, 2H).

Synthesis of poly(ε-caprolactone-*co*-α-triiodobenzoate-ε-caprolactone) (PCL-TIB)

In a typical experiment (Table 1, sample PCL-TIB$_8$), PCL (17.5 mmol of CL unit, 2 g) was dissolved in anhydrous THF (300 mL) in a four-necked reactor equipped with a mechanical stirrer and kept at −40 °C under argon atmosphere. A solution of LDA (0.25 eq./CL unit, 2.2 mL) was injected with a syringe through a septum and the mixture was kept at −50 °C under stirring for 30 min. After this activation step, TIBC (0.25 eq./CL unit, 2.3 g) was added, the mixture was kept under stirring and maintained at −40 °C. After 30 min, the reaction was stopped by addition of a saturated solution of NH$_4$Cl (100 mL) and pH was adjusted to 7 with 1 M HCl. The polymer was extracted with dichloromethane (3 × 150 mL). The combined organic phases were washed three times with distilled water (3 × 150 mL), dried on anhydrous MgSO$_4$ and filtered. After partial solvent evaporation under reduced pressure, the polymer was recovered by precipitation in cold methanol and dried overnight under vacuum. The polymer was obtained with an average yield of 85% and 8% substitution with respect to CL units (ESI Fig. S3†).

^{1}H NMR: (300 MHz; CDCl$_3$): δ (ppm) = 8.3 and 7.6 (2H, C*H*), 4.0 (2H, C*H*$_2$–O), 2.3 (2H, C(O)C*H*$_2$), 1.6 (4H, C(O)CH$_2$–C*H*$_2$–CH$_2$–C*H*$_2$–CH$_2$–O), 1.4 (2H, C(O)CH$_2$–CH$_2$–C*H*$_2$–CH$_2$–CH$_2$–O).

Tensile tests

Sample plates were prepared by dissolution of the polymer blends in dichloromethane followed by solvent evaporation under atmospheric pressure and in dark. Mechanical properties of the polymers were determined by performing tensile mechanical tests on dogbone-style tensile specimens ($\approx 15 \times 2 \times 0.5$ mm^3, section = 1×10^{-6} m^2, ESI Fig. S6†) at 37 °C with GABO Eplexor® 1500 N testing machine equipped with a 25 N cell force at a crosshead speed rate of 5 mm min^{-1}. Each sample was analyzed in triplicate and Young's modulus (E, MPa), and yield strain (Y, %) were expressed as the mean value of the three measurements. E was calculated using the initial linear portion of the stress/strain curves.

Polymer blends preparation

Two types of polymer blends were prepared and used to yield sample films with 0.5 mm thickness. Films were prepared by solvent evaporation method in acetone and used for X-ray imaging tests. First series of blends consisted of PCL-TIB and pristine PCL and were prepared for *in vitro* evaluation of PCL-TIB/PCL blends radio-opacity with respect to aluminum wedge reference. Weight ratios of PCL-TIB and PCL were

Table 1 Conditions for the synthesis of poly(ε-caprolactone-*co*-α-triiodobenzoate-ε-caprolactone) (PCL-TIB) from commercial PCL (M_n = 32 000 g mol^{-1}; $Đ$ = 1.8)

Sample	Temperature (°C)	LDA eq.	CTIB eq.	SD (%)	M_n (g mol^{-1})	$Đ$	Distribution
PCL-TIB$_{3.5}$	−50	0.5	0.25	3.5	24 000	1.7	Monomodal
PCL-TIB$_8$	−40	0.25	0.25	8	19 000	2.6	Monomodal
PCL-TIB$_{12}$	−30	0.25	0.25	12	17 000	3.8	Weak shoulder
PCL-TIB$_{24}$	−30	0.5	0.5	24	9500	4.5	Bimodal

adjusted to yield polymer blends containing 0, 5, 10, 15, and 25 wt% of iodine, which corresponds to PCL-TIB weight ratios in blends of 0 wt%, 25 wt% PCL-TIB$_8$, 50 wt% PCL-TIB$_8$, 55 wt% PCL-TIB$_{12}$ and 95 wt% PCL-TIB$_{12}$, respectively.

Second series of blends was prepared from PCL-TIB and PLA$_{50}$-*b*-PEG-*b*-PLA$_{50}$ (central block PEG = 20 000 g mol^{-1}; side blocks PLA$_{50}$ = 175 000 g mol^{-1}) to evaluate *ex vivo* the potential of PCL-TIB as macromolecular radio-opacifier at various weight ratios. PLA$_{50}$-PEG-PLA$_{50}$ with a high molecular weight (370 000 g mol^{-1}) was chosen as a non-X-rays visible resorbable thermoplastic model because it previously demonstrated interest as drug releasing coatings, drug releasing microparticles or as biomaterial to generate scaffolds for skin tissue engineering.[47–49] Ratios of PCL-TIB and PLA$_{50}$-PEG-PLA$_{50}$ were adjusted to yield polymer blends containing 0, 1, 2.5, 5, 10 and 20 wt% of iodine, which corresponds to PCL-TIB weight ratios in blends of 0 wt% PCL-TIB, 10 wt% PCL-TIB$_{3.5}$, 25 wt% PCL-TIB$_{3.5}$, 50 wt% PCL-TIB$_{3.5}$, 50 wt% PCL-TIB$_8$ and 100 wt% PCL-TIB$_8$, respectively.

In vitro X-ray imaging

X-radiographs were obtained using a standard Elitys X-ray machine (Trophy radiology) kindly made available by M. Guilhem Romieu dentist in Prades-Le-Lez, France. Imaging parameters were as follow: sample-amplifier distance 5 cm, angle 90°, 70 kV, 4 mA, 0.1 s. Relative radio-opacity of samples was calculated by image analyses with respect to aluminum wedge of the same thickness. For this purpose, an aluminum scale with thicknesses ranging from 0.5 to 5.5 mm was used. Each image was analyzed using ImageJ software to determine the sample grey index (GI). For each sample, GI was measured in various locations (between 6 to 10) and was then expressed as mean value ± standard deviation. GI scored on a 255-unit scale with white = 255 and black = 0. The X-ray absorbance ranged from 0% (no X-ray absorption) to 100% (full absorption) and was determined using eqn (1).

$$A(\%) = 100 \times \left(1 - \left(\frac{GI_{Al} - GI_s}{255}\right)\right) \tag{1}$$

with A being the percentage of absorbance, GI_s the grey index of sample and GI_{Al} the grey index of aluminum wedge.

Ex vivo X-ray imaging

X-radiographs were obtained using a standard clinical Trixell X-ray machine (Moirans, France) with Surgivisiotractor interface. Imaging parameters were as follow: sample-amplifier distance 50 cm, angle 90°, 40 kV, 30 mA s^{-1}, 1 s. Chicken breast muscle (4 cm thickness) was chosen as an anatomic *ex vivo* model. This model was transected longitudinally in the middle and samples were placed in cutting area at a depth of *ca.* 2 cm from the muscle surface. To evaluate the influence of degradation time on X-ray visibility, control plate at 0 wt% iodine and sample plates at 10 and 20 wt% iodine were placed in 8 mL of PBS (pH 7.4) at constant temperature (37 °C) under stirring for 6 weeks (stirring speed of 100 rpm). Degraded samples were then analyzed as described above. A 2 mm thick aluminum wedge placed next to the anatomic model was imaged with the samples and used as positive control.

Cytocompatibility

Mouse L929 fibroblasts (L929) were cultured in modified Eagle's medium (MEM) containing 10% horse serum, penicillin (100 µg mL^{-1}), streptomycin (100 µg mL^{-1}), and glutamax (1%). For each sample, three plates were punched out from the same PCL-TIB sample. Plates were disinfected in ethanol for 30 minutes before being immersed in a solution of sterile PBS containing penicillin and streptomycin (1 mg mL^{-1}) and incubated for 48 h at 37 °C. The plates were then rinsed 3 times with sterile PBS before being soaked for 12 hours in sterile PBS. These sterile PCL-TIB plates were stamped to fit the wells of 24-well cell culture plates. *In vitro* cytocompatibility was assessed by monitoring the proliferation of L929 fibroblasts on the surface of the plates. To do this, the plates were placed in polystyrene 24-well tissue culture plates (TCPS) and seeded with 1×10^4 L929 cells. Cell viability after 1, 2 and 3 days was evaluated using the PrestoBlue™ assay that reflects the number of living cells present on a surface at a given time point. Culture medium was removed at scheduled time points and replaced by 1 mL of fresh medium containing 10% PrestoBlue™. Fluorescence at λ = 530 nm(λ_{ex}) and λ = 615 nm(λ_{em}) was measured on a Victor X3 photometer (Perkin-Elmer). All data points and standard deviations correspond to measurements in triplicate.

Results and discussion

Synthesis of radiopaque PCL

One reported way for preparing X-ray radiopaque PCL is the ring opening copolymerization of ε-CL with functional ε-CL bearing heavy atoms like iodine. This strategy was followed by our group in the recent past to yield poly(α-iodo-ε-caprolactone-*co*-ε-caprolactone).[41,42] Speaking of materials however, the synthesis of functional lactones does not appear as a convenient strategy as

large amounts of products can barely be obtained. To overcome this limitation our group developed few years ago an anionic post-modification reaction that provided various functional PCLs with 5 to 15% of functional groups including poly(α-iodo-ε-caprolactone-*co*-ε-caprolactone) (PCL-I).[40] In the case of PCL-I, low stability of the aliphatic carbon–iodine bond was encountered, which led to a rapid loss of X-ray visibility. With the aim to prepare a more stable radiopaque PCL suitable for implantation, the anionic post-polymerization modification strategy has been applied to yield PCL bearing triiodobenzoyl groups (PCL-TIB). Another expected advantage of TIB substitution compared to direct iodine substitution is the higher iodine content that is reachable for the same degree of substitution of the PCL backbone. PCL-TIB being designed a radio-opacifier additive, this increase is of benefit as less PCL-TIB should be required to induce X-ray visibility, which should guaranty minimal impact on the polymer matrix properties.

Scheme 1 summarizes the synthesis of PCL-TIB. Triiodobenzoyl chloride (TIBC) was first prepared as an activated intermediate in a 60% yield (ESI Fig. S1 and S2†). TIBC was then reacted with PCL under anionic chemical modification conditions. The parameters of the PCL activation step with LDA and of the subsequent substitution with TIBC have been chosen in order to guaranty visibility while minimizing side reactions including backbone hydrolysis. Each step was run for 30 minutes, while the number of reactant equivalents and the temperature were varied (Table 1). The polymer chemical structure was characterized by ^{1}H-NMR (ESI Fig. S3†). Substitution degree (SD) was calculated using eqn (2) by comparison of the integrations of the well-defined resonance peaks at 8.3 ppm and 7.6 ppm, corresponding to the aromatic protons of TIB group, with the integration of the resonance peak at 4.0 ppm, corresponding to a methylene of PCL.

$$\text{SD} (\%) = I_{8.3-7.6\text{ppm}}/(I_{4\text{ppm}}/2) \times 100 \qquad (2)$$

Depending on the reaction conditions a substitution degree ranging from 3.5% to 24% was obtained. As classically observed for this type of reaction, a strong impact on the molecular weight and dispersity was also observed. In more details, whereas the lowest SD of 3.5% could be obtained with
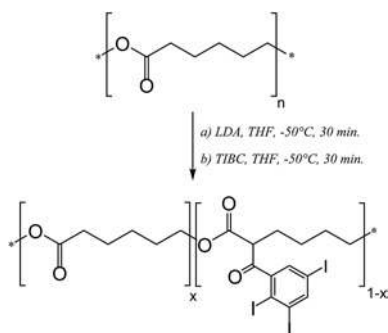
a minimal impact on the molecular weight and dispersity ($M_n \approx 24\,000$ g mol^{-1} and $Đ = 1.7$) compared to pristine PCL ($M_n \approx 32\,000$ g mol^{-1} and $Đ = 1.8$) (Fig. 1), a further increase of SD clearly had a strong impact on these macromolecular parameters (Table 1). In particular, for the highest SDs, a shoulder (PCL-TIB$_{12}$) or even bimodality (PCL-TIB$_{24}$) were observed on the chromatograms (not shown). For that reason, PCL-TIB$_{24}$ was not further considered in this work and PCL-TIB$_{12}$ was only used in the preliminary *in vitro* visibility assessments. It is to note that molecular weight decrease is classically observed with the anionic activation of polyester, as a consequence of hydrolysis and backbiting side reactions. However, although remarkable in terms of influence on the final molecular weight, the observed decrease only corresponds to a very low extent of side reactions. It represents less than 0.2% hydrolysis of the ester groups initially present in the polymer chain in the case of the lower SD, *i.e.* PCL-TIB$_{3.5}$, and *ca.* 0.7% hydrolysis for PCL-TIB$_{12}$. In addition, this drawback should be put in perspective with a major advantage of the approach, that is, starting from commercially available PCL this one pot and time saving reaction allows the preparation of *ca.* 2 g batches of PCL-TIB in a single day, including reaction and purification.

Thermal properties of monomodal PCL-TIB were studied by DSC and TGA and results are reported in Table 2. Melting temperatures of PCL-TIB$_{3.5}$ were *ca.* 10 °C lower than the ones of pristine PCL with $T_{m_1} = 52$ °C and $T_{m_2} = 49$ °C for PCL-TIB$_{3.5}$ against $T_{m_1} = 62$ °C and $T_{m_2} = 57$ °C for PCL. The same observation was done on crystallization temperature, which is 17 °C for PCL-TIB$_{3.5}$ against 23 °C for PCL. Similar results were obtained with PCL-TIB$_8$ with as expected lower crystallinity and lower crystallization temperature compared to PCL-TIB$_{3.5}$. These differences can be ascribed to the lower molecular weight of PCL-TIB compared to pristine PCL, as well as a lower crystallinity due to chains packing disturbance resulting from the TIB side group. This lower crystallinity is confirmed by the melting enthalpy values measured that are *ca.* twice lower for PCL-TIB compared to PCL. With aim to compare stability of PCL-I and PCL-TIB, thermogravimetric analyses were conducted on radiopaque PCLs with a similar iodine molar content of 10%, PCL-TIB$_{3.5}$ and PCL-I$_{10}$ (SD = 10%), that was synthesized according to the procedure previously reported.[40] Thermograms (ESI Fig. S4†) showed that PCL-TIB$_{3.5}$ thermal degradation
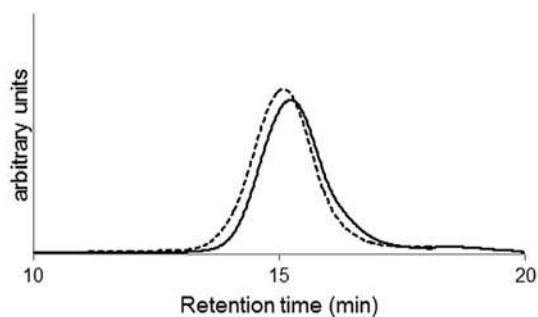

Scheme 1 Synthetic scheme for the preparation of poly(ε-caprolactone-*co*-α-triiodobenzoate-ε-caprolactone) (PCL-TIB).

Fig. 1 SEC chromatograms of PCL (dashed line) and PCL-TIB$_{3.5}$ (plain line).

Table 2 PCL-TIB thermal properties

Sample	T_g (°C)	$T_{m_1}/\Delta H_{m_1}$ (°C; J g^{-1})	$T_{m_2}/\Delta H_{m_2}$ (°C; J g^{-1})	T_c (°C)
PCL	<-60 °C	62/113	57/78	23
PCL-TIB$_{3.5}$	<-60 °C	52/60	49/44	17
PCL-TIB$_8$	<-60 °C	52/44	48/41	12

Fig. 2 Pictures of PCL-TIB/PLA$_{50}$-b-PEG-b-PLA$_{50}$ blends with increasing contents of PCL-TIB. Percentages correspond to iodine weight ratios.

occurred in the same range of temperature than for PCL with an onset temperature around 270 °C against 260 °C. Under the same conditions PCL-I degraded much earlier than PCL-TIB with an onset temperature found at *ca.* 205 °C and degradation temperatures $T_{d5\%}$ found at 269 °C for PCL-I against 296 °C for PCL-TIB. This result confirms the higher thermal stability of PCL-TIB *vs.* PCL-I.

In vitro X-ray imaging of PCL-TIB/PCL blends

As a first evaluation of PCL-TIB as radio-opacifier for X-ray imaging, blends of PCL and PCL-TIB were prepared. Defined quantities of PCL-TIB substituted at 8% and 12% were used to yield final iodine weight contents ranging from 0 to 25 wt%. Films with a thickness of 0.5 mm were imaged using Elitys (Trophy radiology) equipment (ESI Fig. S5†) and compared with an aluminum wedge of the same thickness. Grey index (scored on a 255-unit scale with white = 255 and black = 0), relative absorption and attenuation per μm were calculated based on the X-ray images analyses and are listed in Table 3. Note that images were measured simultaneously, that is, grey values can be compared. A quasi-linear evolution of GI with respect to iodine weight percentage was obtained. Similar GI, and therefore attenuation per μm thickness, was obtained for the aluminum wedge and the PCL/PCL-TIB blend with as low as 15 wt% iodine. This result demonstrates the ability of PCL-TIB to induce X-ray absorption when used in polymer blends.

Visual and mechanical evaluations of PCL-TIB/PLA$_{50}$-b-PEG-b-PLA$_{50}$ blends

To further evaluate the potential of PCL-TIB as radio-opacifier for X-ray imaging, blends of PLA$_{50}$-b-PEG-b-PLA$_{50}$ and

PCL-TIB were prepared. Custom made PLA$_{50}$-b-PEG-b-PLA$_{50}$ copolymer was chosen as it was successfully used by our group to formulate drug releasing coatings and drug releasing microparticles, or to generate scaffolds for skin tissue engineering.[47–49] Considering the variety of applications for this family of copolymers, it appears therefore as a good candidate for blending and radio-opacifying with PCL-TIB. Again, defined quantities of PCL-TIB substituted at 3.5% or 8% were used to yield final iodine weight contents ranging from 0 to 20 wt%. The films obtained are shown in Fig. 2. Homogeneous films were obtained for low and high PCL-TIB contents (1, 2.5 and 20 wt% iodine). In opposition, macroscopic phase separation was observed for PCL-TIB contents corresponding to 5 wt% iodine (50 wt% PCL-TIB$_{3.5}$) and 10 wt% iodine (50 wt% PCL-TIB$_8$). Although PCL-TIB was present in the all sample, as demonstrated by the clear yellow color of the film, areas of higher PCL-TIB concentrations were observed under the form of brown spots. This result highlights a lower compatibility of the tri-block copolymer and PCL-TIB when a 1 : 1 mass ratio is used. It is to note that phase separation was not observed in PCL blends, whatever the PCL-TIB concentration, which underlines the importance of the nature of polymers to be used in the blend, as well as the PCL-TIB/polymer ratio.

The impact of PCL-TIB$_{3.5}$ on the mechanical properties of the blends was then assessed. The tensile tests were performed on dogbone-style tensile specimens (ESI Fig. S6†). Blends with the

Table 3 Comparison of *in vitro* X-ray absorptions of PCL-TIB/PCL blends (0.5 mm thickness) and of aluminum wedge (0.5 mm thickness)

Iodine content (wt%)	Grey index	Relative absorption^a (%)	Attenuation^b (%) per μm thickness
0	15 ± 3	25	0.011
5	26 ± 7	43	0.020
10	33 ± 8	55	0.025
15	64 ± 9	107	0.050
25	82 ± 7	136	0.065
Aluminum wedge	60 ± 8	100	0.047

^{a} Calculated with respect to grey index of the aluminum wedge. ^{b} Calculated based on the grey index scale with white = 255 and black = 0.
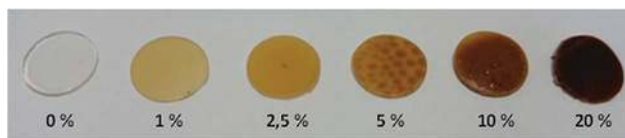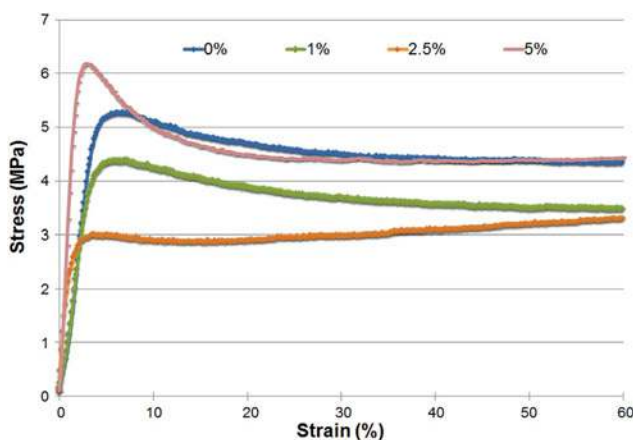

Fig. 3 Typical stress-strain tensile curves of PCL-TIB/PLA$_{50}$-b-PEG-b-PLA$_{50}$ blends (GABO Eplexor® 1500 N testing machine, 25 N cell force, 5 mm min^{-1} crosshead speed rate, 37 °C). Percentages correspond to iodine weight ratios; samples were not loaded to failure.
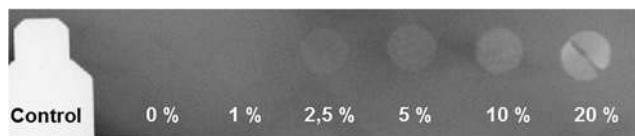
Fig. 4 *Ex vivo* X-ray images of PCL-TIB/PLA$_{50}$-*b*-PEG-*b*-PLA$_{50}$ blends implanted in a 4 cm thick anatomical model. Control corresponds to 2 mm thick aluminum wedge. Percentages correspond to iodine weight ratios (20 wt% sample film shown is broken in two pieces; dark line in the middle of the sample corresponds to this fracture).

highest PCL-TIB content were too fragile and were therefore not tested. The other samples (1 to 5 wt% iodine) were all prepared with the same PCL-TIB$_{3.5}$ and were not loaded to failure as they present a rupture strain greater than the possibility of the testing machine. Typical tensile curves are shown in Fig. 3. The results present the nominal stress (force divided by the initial section) in function of strain (displacement divided by the initial length). The curves present an initial linear curve that can be assimilated to the elasticity of the material. The Young modulus is evaluated by fitting this part of the curve. The yield strain is defined as the end of this linear part. The values of the Young modulus and the yield strain are listed in Table 4. The increasing content of PCL-TIB seems to increase the stiffness of the material by increasing the Young modulus and reducing the yield strain. After the elastic part, the curves are very flat seeming to a creep test with an increasing deformation with a constant stress. It is to note that increasing contents of PCL-TIB$_{3.5}$ (if iodine content is no greater than 5 wt%) do not change significantly the mechanical behavior of the PLA$_{50}$-*b*-PEG-*b*-PLA$_{50}$ with similar strain-stress curves profiles and characteristic values in a same range.

Ex vivo X-ray imaging of PCL-TIB/PLA$_{50}$-*b*-PEG-*b*-PLA$_{50}$ blends

The radio-opacifying effect of PCL-TIB in the PCL-TIB/PLA$_{50}$-*b*-PEG-*b*-PLA$_{50}$ blends was evaluated under conditions mimicking implantation. Radiopaque sample films with 0.5 mm thickness were inserted in chicken breast muscle that was chosen as anatomical *ex vivo* model. All samples were then imaged the same day under the same conditions (see experimental parts for details). It is first important to note that PLA$_{50}$-*b*-PEG-*b*-PLA$_{50}$ sample without PCL-TIB did not demonstrate any additional X-ray absorption compared to the surrounding tissue (Fig. 4). It is to note that X-ray absorption of anatomical model was not nil as shown by the greyish color of tissues and the calculated absorption of 50% (Table 4).

In opposition, all samples containing PCL-TIB exhibited a clear contrast and were visible in the anatomical model. Remarkably, even iodine content in the blend as low as 1 wt% made the sample visible. This visibility was however considered too weak by surgeons for practical use. An iodine content of 2.5 wt% is therefore the lowest one with respect to practical clinical imaging. Little difference between blends containing 2.5 and 5 wt% iodine was observed in this X-ray imaging experiment. This was due to the inhomogeneity of muscle and

Table 4 Mechanical properties and percentage of X-ray absorption of polymer blends samples (600 μm thickness) *ex vivo* before and after degradation

Iodine content (wt%)	E (MPa)	Y (%)	Absorption at $t_0{}^{a,b}$ (%)	Delta absorption at 6 weeks^{a,c} (%)
Muscle	—	—	47	0
0	0.8	5.2	50	0
1	0.9	4.2	52	nd
2.5	2.4	2.3	55	nd
5	2.9	3.3	55	nd
10	nd	nd	58	−0.4
20	nd	nd	73	−0.4
Aluminum wedge	—	—	96	—

^{a} Calculated based on the grey index scale with white = 255 (100% absorption) and black = 0 (0% absorption). ^{b} Image used for the analyses is shown in Fig. 4 ^{c} Image used for the analyses is shown in Fig. 5

of the above mentioned inhomogeneity of the 5 wt% blend that is visible in Fig. 4 and emphasized in Fig. S7 (ESI Fig. S7†) with clear isolated spots exhibiting higher contrast compared to the rest of the sample. Samples with 10 and 20 wt% iodine were obviously the most visible and exhibited X-ray absorption of 60% and 76%, respectively, compared to the 2 mm thick aluminum wedge. This result confirms that image contrast is proportional to the amount of iodine.

Stability of X-ray visibility over time was assessed using aged sample plates containing 0, 10 or 20 wt% iodine. Samples were placed for 6 weeks in PBS at 37 °C under stirring to mimic physiological conditions prior to implantation in an anatomical model for X-ray imaging. The non-degraded samples were implanted in the same anatomical model for comparison (Fig. 5). Degraded samples remained highly visible after 6 weeks. In addition, no difference of contrast was found between the degraded and non-degraded samples. A negligible variation of X-ray absorption (0.4%) was calculated from the GI values. These results confirm the high stability of the carbon–iodine bond in PCL-TIB and the potential of this copolymer to
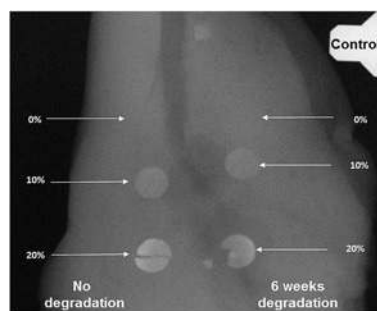

Fig. 5 *Ex vivo* X-ray images of non-degraded (left-hand side) and degraded (right-hand side) PCL-TIB/PLA$_{50}$-*b*-PEG-*b*-PLA$_{50}$ blends sample plates implanted in a 4 cm thick anatomical model. Control corresponds to 2 mm thick aluminum wedge. Percentages correspond to iodine weight ratios.

be used as macromolecular radio-opacifier for implantable medical devices.

Cytocompatibility of radiopaque PCL-TIB/PLA$_{50}$-*b*-PEG-*b*-PLA$_{50}$ blends

X-ray absorption capability is the main parameter to consider PCL-TIB as a potential macromolecular radio-opacifying agent. However, in the frame of medical applications and implantable medical devices, another critical parameter is the biocompatibility of the biomaterial towards tissues and cells. For that reason, and as a first approach, an evaluation of cells proliferation was performed on films to assess the cytocompatibility of PCL-TIB/PLA$_{50}$-*b*-PEG-*b*-PLA$_{50}$ blends and to determine whether they are suitable for cell culture and cell-contacting biomedical applications. Tests were conducted on the L929 fibroblast cell line, as recommended by International and European standards (ISO 10993-5:2009). Films with iodine contents in the range 1–5 wt% were tested. Fig. 6 shows the proliferation at 1, 3 and 7 days of L929 murine fibroblasts on the radiopaque blends compared to pure PLA$_{50}$-*b*-PEG-*b*-PLA$_{50}$ (0 wt% iodine) and TCPS positive control. L929 fibroblasts adhered and proliferated on the samples. In more details, following an initial period up to 3 days with limited proliferation for all samples and controls, fast proliferation was then observed. As expected, proliferations on blends were slower than on TCPS positive control, but were significant with relative proliferations in the range 70–84% for blends containing 2.5 wt% and 5 wt%, respectively. It is of importance to note that cells proliferation was better on PCL-TIB/PLA$_{50}$-*b*-PEG-*b*-PLA$_{50}$ blends compared to PLA$_{50}$-*b*-PEG-*b*-PLA$_{50}$ and was improved with increasing PCL-TIB contents. This is remarkable considering that block copolymers of PLA and PEG are widely recognize as cytocompatible materials and have a long track record as biomaterials. This result confirms that PCL-TIB appears to be suitable for the growth of fibroblasts and cell-contacting applications and may be of interest for the design of X-ray visible medical devices.
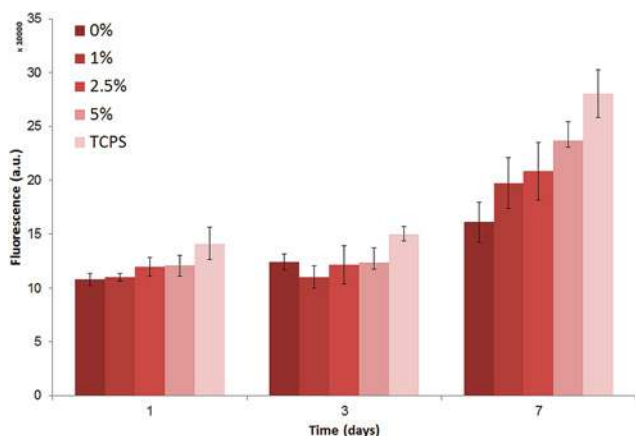

Fig. 6 L929 fibroblasts proliferation on PCL-TIB/PLA$_{50}$-*b*-PEG-*b*-PLA$_{50}$ blends (1 to 5 wt% iodine) compared to pristine PCL films (0 wt% iodine) and TCPS control at 1, 3, and 7 days (data are expressed as means ± SD and correspond to measurements in triplicate).

Conclusions

Poly(ε-caprolactone-*co*-α-triiodobenzoate-ε-caprolactone) (PCL-TIB) was synthesized with substitution ratios ranging from 3.5 to 24%. This family of macromolecular X-ray contrast agents could be blended in (co)polyester matrices to induce X-ray opacity. Mechanical properties of the blends with up to 5 wt% iodine were not significantly impacted by PCL-TIB$_{3.5}$ compared to the raw polymer matrices. Radio-opacity was observed in *ex vivo* model with 1 wt% iodine although for practical use a 2.5 wt% should be preferred. In addition, PCL-TIB was shown to be stable enough to make blends radiopaque, even after 6 weeks degradation, and compatible with L929 fibroblasts proliferation. In conclusion, PCL-TIB copolymers appear to be promising candidates as additive for implantable medical devices requiring X-ray imaging abilities.

Acknowledgements

References

1 S. M. Janib, A. S. Moses and J. A. MacKay, *Adv. Drug Delivery Rev.*, 2010, **62**, 1052–1063.

2 B. Nottelet, V. Darcos and J. Coudane, *Eur. J. Pharm. Biopharm.*, 2015, DOI: 10.1016/j.ejpb.2015.06.023.

3 Z. Y. Wang, T. Chang, L. Hunter, A. M. Gregory, M. Tanudji, S. Jones and M. H. Stenzel, *Aust. J. Chem.*, 2014, **67**, 78–84.

4 N. Anton and T. F. Vandamme, *Pharm. Res.*, 2014, **31**, 20–34.

5 S. Dawlee, A. Jayakrishnan and M. Jayabalan, *J. Mater. Sci.: Mater. Med.*, 2009, **20**, 243–250.

6 S. Kiran, N. R. James, R. Joseph and A. Jayakrishnan, *Biomaterials*, 2009, **30**, 5552–5559.

7 M. Marcos, P. Cano, P. Fantazzini, C. Garavaglia, S. Gomez and L. Garrido, *Magn. Reson. Imaging*, 2006, **24**, 89–95.

8 F. Hallouard, S. Briancon, N. Anton, X. Li, T. Vandamme and H. Fessi, *J. Pharm. Sci.*, 2013, **102**, 4150–4158.

9 F. Hallouard, S. Briancon, N. Anton, X. Li, T. Vandamme and H. Fessi, *Pharm. Res.*, 2013, **30**, 2023–2035.

10 V. P. Torchilin, *Adv. Drug Delivery Rev.*, 2002, **54**, 235–252.

11 A. J. L. Villaraza, A. Bumb and M. W. Brechbiel, *Chem. Rev.*, 2010, **110**, 2921–2959.

12 M. Vert, *Prog. Polym. Sci.*, 2007, **32**, 755–761.

13 M. Vert, *J. Mater. Sci.: Mater. Med.*, 2009, **20**, 437–446.

14 B. Nottelet, C. Di Tommaso, K. Mondon, R. Gurny and M. Moller, *J. Polym. Sci., Part A: Polym. Chem.*, 2010, **48**, 3244–3254.

15 M. A. Woodruff and D. W. Hutmacher, *Prog. Polym. Sci.*, 2010, **35**, 1217–1256.

16 B. C. Thanoo, M. C. Sunny and A. Jayakrishnan, *Biomaterials*, 1991, **12**, 525–528.

17 B. C. Thanoo and A. Jayakrishnan, *Biomaterials*, 1990, **11**, 477–481.

18 F. Luderer, I. Begerow, W. Schmidt, H. Martin, N. Grabow, C. M. Buenger, W. Schareck, K.-P. Schmitz and K. Sternberg, *J. Biomater. Appl.*, 2013, **28**, 219–231.

19 C. Shasteen, S. M. Kwon, K. Y. Park, S. Y. Jung, S. H. Lee, C. G. Park, M. H. Kim, S. Kim, W.-C. Son, T. H. Choi and Y. B. Choy, *J. Biomed. Mater. Res., Part B*, 2013, **101**, 320–329.

20 T. Lamsa, H. Jin, J. Mikkonen, J. Laukkarinen, J. Sand and I. Nordback, *Pancreatology*, 2006, **6**, 301–305.

21 I. Nordback, S. Raty, J. Laukkarinen, S. Jarvinen, A. Piironen, J. Leppiniemi, M. Kellomaki and J. Sand, *Pancreatology*, 2012, **12**, 264–271.

22 L. Mazzocchetti, M. Scandola and A. Pollicino, *Polymer*, 2008, **49**, 5215–5224.

23 L. Mazzocchetti, E. Cortecchia and M. Scandola, *ACS Appl. Mater. Interfaces*, 2009, **1**, 726–734.

24 J. L. Pariente, L. Bordenave, R. Bareille, C. Ohayon-Courtes, C. Baquey and M. Le Guillou, *Biomaterials*, 1999, **20**, 523–527.

25 W. Wang, J. Liu, C. Li, J. Zhang, J. Liu, A. Dong and D. Kong, *J. Mater. Chem. B*, 2014, **2**, 4185–4192.

26 D. Mawad, H. Mouaziz, A. Penciu, H. Mehier, B. Fenet, H. Fessi and Y. Chevalier, *Biomaterials*, 2009, **30**, 5667–5674.

27 F. Mottu, D. A. Rufenacht, A. Laurent and E. Doelker, *Biomaterials*, 2002, **23**, 121–131.

28 A. Galperin and S. Margel, *Biomacromolecules*, 2006, **7**, 2650–2660.

29 D. Horak, M. Metalova and F. Rypacek, *J. Biomed. Mater. Res.*, 1997, **34**, 183–188.

30 M. A. B. Kruft, A. Benzina, F. Bar, F. H. Vanderveen, C. W. M. Bastiaansen, R. Blezer, T. Lindhout and L. H. Koole, *J. Biomed. Mater. Res.*, 1994, **28**, 1259–1266.

31 M. A. B. Kruft, A. Benzina, R. Blezer and L. H. Koole, *Biomaterials*, 1996, **17**, 1803–1812.

32 N. Moszner, U. Salz, A. M. Klester and V. Rheinberger, *Angew. Makromol. Chem.*, 1995, **224**, 115–123.

33 K. Saralidze, Y. B. J. Aldenhoff, M. L. W. Knetsch and L. H. Koole, *Biomacromolecules*, 2003, **4**, 793–798.

34 B. Vazquez, M. P. Ginebra, F. J. Gil, J. A. Planell, A. L. Bravo and J. San Roman, *Biomaterials*, 1999, **20**, 2047–2053.

35 C. Zaharia, T. Zecheru, M. F. Moreau, F. Pascaretti-Grizon, G. Mabilleau, B. Marculescu, R. Filmon, C. Cincu, G. Staikos and D. Chappard, *Acta Biomater.*, 2008, **4**, 1762–1769.

36 N. R. James, J. Philip and A. Jayakrishnan, *Biomaterials*, 2006, **27**, 160–166.

37 S. Kiran, N. R. James, A. Jayakrishnan and R. Joseph, *J. Biomed. Mater. Res., Part A*, 2012, **100**, 3472–3479.

38 M. D. Hindenlang, A. A. Soudakov, G. H. Imler, C. T. Laurencin, L. S. Nair and H. R. Allcock, *Polym. Chem.*, 2010, **1**, 1467–1474.

39 K. A. Aamer, K. L. Genson, J. Kohn and M. L. Becker, *Biomacromolecules*, 2009, **10**, 2418–2426.

40 B. Nottelet, J. Coudane and M. Vert, *Biomaterials*, 2006, **27**, 4948–4954.

41 S. El Habnouni, S. Blanquer, V. Darcos and J. Coudane, *J. Polym. Sci., Part A: Polym. Chem.*, 2009, **47**, 6104–6115.

42 S. El Habnouni, V. Darcos and J. Coudane, *Macromol. Rapid Commun.*, 2009, **30**, 165–169.

43 T. R. Olsen, L. L. Davis, S. E. Nicolau, C. C. Duncan, D. C. Whitehead, B. A. Horn and F. Alexis, *Acta Biomater.*, 2015, **20**, 94–103.

44 C. Rode, A. Schmidt, R. Wyrwa, J. Weisser, K. Schmidt, N. Moszner, R. P. Gottlober, K. Heinemann and M. Schnabelrauch, *Polym. Int.*, 2014, **63**, 1732–1740.

45 L. Sang, Z. Y. Wei, K. L. Liu, X. H. Wang, K. D. Song, H. Wang and M. Qi, *J. Biomed. Mater. Res., Part A*, 2014, **102**, 1121–1130.

46 A. L. Carbone, M. Song and K. E. Uhrich, *Biomacromolecules*, 2008, **9**, 1604–1612.

47 X. Garric, O. Guillaume, H. Dabboue, M. Vert and J. P. Moles, *J. Biomater. Sci., Polym. Ed.*, 2012, **23**, 1687–1700.

48 A. K. Jain, A. K. Goyal, N. Mishra, B. Vaidya, S. Mangal and S. P. Vyas, *Int. J. Pharm.*, 2010, **387**, 253–262.

49 M. Morille, V. T. Tran, X. Garric, J. Cayon, J. Coudane, D. Noel, M. C. Venier-Julienne and C. N. Montero-Menei, *J. Controlled Release*, 2013, **170**, 99–110.